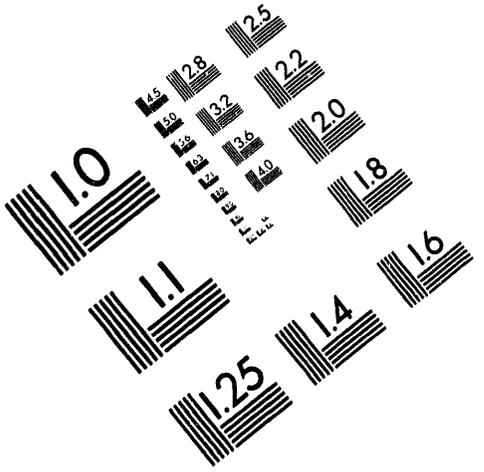

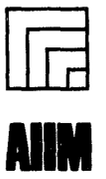

Association for Information and Image Management
1100 Wayne Avenue, Suite 1100
Silver Spring, Maryland 20910
301/587-8202

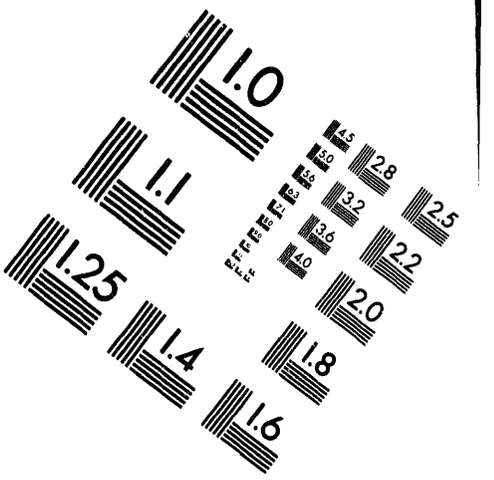

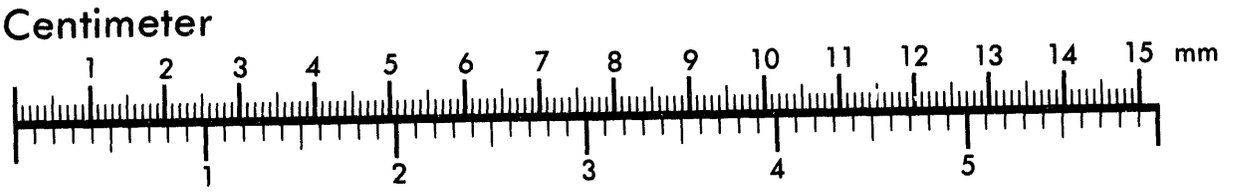

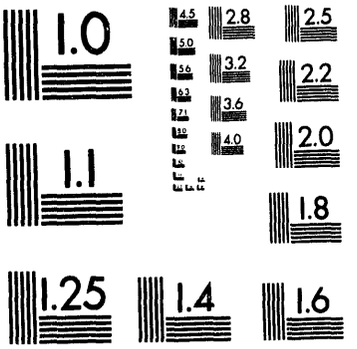

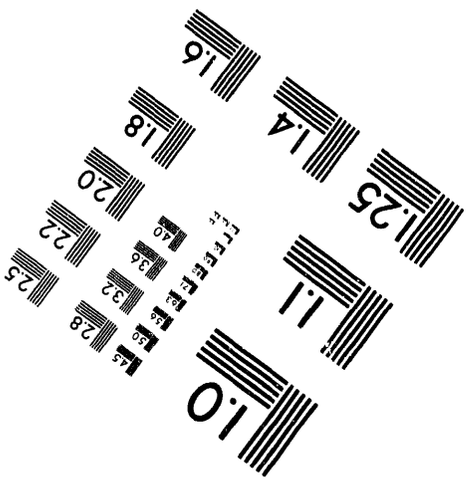

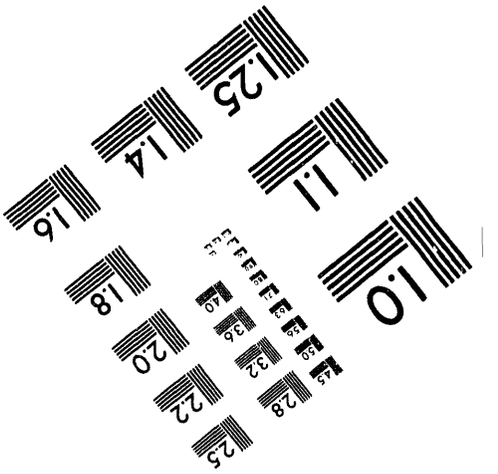

MANUFACTURED TO AIIM STANDARDS
BY APPLIED IMAGE, INC.

1 of 1

Thermal Decomposition of CH_2Cl_2

by

K. P. Lim and J. V. Michael
Chemistry Division, Argonne National Laboratory, Argonne, IL 60439, USA

Corresponding Author:

Dr. J. V. Michael
D-183, Bldg 200
Argonne National Laboratory
Argonne, IL 60439
Phone: (708) 252-3171 Fax: (708) 252-4470
E-mail: Michael@ANLCHM.BITNET

(25th Symp. (Int'l) on Combust., Submitted Oct., 1993)

Desired Presentation: Oral
Preferred Publication: Proceedings
Code Letter: **E,A** Code Numbers: **1.1, 1.5**

	Text	Reference	Tables	Figures	Total
Count	3045 words	27 citations	3.5 pages	6 pages	
Equiv. Words	3045	502	800	1200	5547

(Not Patentable)

This work was supported by the U. S. Department of Energy, Office of Basic Energy Sciences, Division of Chemical Sciences, under Contract No. W-31-109-Eng-38.

Abstract

The thermal decomposition of CH_2Cl_2 has been investigated in reflected shock waves experiments at temperatures between 1400-2300 K and at three different loading pressures with various initial CH_2Cl_2 concentrations. The resulting product Cl-atoms are monitored by the atomic resonance absorption spectrometric (ARAS) technique. A reaction mechanism is used to numerically simulate the measured Cl-atom profiles in order to obtain rate constants for the two primary dissociation reactions: (1) $CH_2Cl_2 \rightarrow CHCl + HCl$ and (2) $CH_2Cl_2 \rightarrow CH_2Cl + Cl$. The experimental second-order Arrhenius expressions for the two reactions are $k_1/[Kr] = 2.26 \times 10^{-8} \exp(-29007\ K/T)$ cm^3 $molecule^{-1}$ s^{-1} and $k_2/[Kr] = 6.64 \times 10^{-9} \exp(-28404\ K/T)$ cm^3 $molecule^{-1}$ s^{-1}, with standard deviations of ±43% and 40%, respectively. The results are compared to theoretical calculations using the semi-empirical Troe formalism. The best fits to the experimental data are obtained with threshold energy and collisional energy transfer parameters of $E^\circ_{10} = 73.0$ kcal $mole^{-1}$ and $\Delta E_{1down} = 630$ cm^{-1}. Similar values for reaction (2) are $E^\circ_{20} = \Delta H^\circ_{20} = 78.25$ kcal $mole^{-1}$ and $\Delta E_{2down} = 394$ cm^{-1}.

INTRODUCTION

Because of needs in incineration strategies for the destruction of chlorocarbon molecules, [1–4] we have studied the thermal decompositions of CH_3Cl, CCl_4, and $COCl_2$ in prior investigations from this laboratory. [5–7] The analytical method used in these studies has been Cl-atom atomic resonance absorption spectrometry (ARAS). The present work on the thermal decomposition of CH_2Cl_2 is a continuation investigation on the chloromethane class of molecules.

The thermal decomposition of CH_2Cl_2 has previously been studied using tubular flow reactors with 1 atm Ar as bath gas by Bozzelli and coworkers. [8,9] Because the initial reactant densities were high in comparison to the present work, a fairly extensive chemical modeling effort with sensitivity analysis was required in this work to explain both the thermal decomposition and subsequent experiments on the oxidation by O_2. The oxidation proceeds after thermal initiation through two possible reactions,

$$CH_2Cl_2 \xrightarrow{k_1} CHCl + HCl \quad (1)$$

$$\xrightarrow{k_2} CH_2Cl + Cl \quad (2)$$

Because there are relatively few prior studies on this and related reactions, Bozzelli and coworkers used best estimates for the thermochemistry of the various species, and subsequently applied Quantum RRK theory [10,11] to calculate some unknown rate constants for use in the chemical model. The obvious question arises as to whether the predictions from theory are in accord with experiment. Because the relative importance of reactions (1) and (2) can be directly assessed by observing both the rate and yields of Cl-atom formation in a dilute system using the ARAS technique, the present study is designed to answer this question.

Measurements of the thermal decomposition of CH_2Cl_2 have been made with three loading pressures in reflected shock wave experiments at low dilution. The measured Cl-atom profiles are explained by considering reactions (1) and (2), and the experimental results for both processes are discussed in terms of Troe type theoretical fits to the data.

EXPERIMENTAL

Apparatus: All experiments were carried out in the reflected shock mode with a shock tube apparatus that has been previously described. [12] Briefly, the shock tube apparatus consisted of two sections: a 7-meter 304 stainless steel tube (i.d. 9.74 cm) and a driver chamber. A thin aluminum diaphragm (4 mil, unscored 1100-H18) separated the two sections. The tube was routinely pumped to $<10^{-8}$ Torr between experiments by an Edwards Vacuum Products, Model CR100P, packaged pumping system. The incident shock velocity was determined from eight pressure transducers (PCB Piezotronics, Inc., Model 1132A) placed at fixed intervals towards the end of the tube. Final temperature and density for each experiment were determined from the incident velocity of the shock front and the initial thermodynamic conditions. Corrections for non-idealities due to boundary layer formation were subsequently applied. [12,13] The photometer system was radially located 6 cm from the endplate and had an optical path length of 9.94 cm. An EMR G14 solar blind photomultiplier tube was used to measured transmittances from the resonance lamp. Transmittances and the differentiated signals from the pressure transducers were recorded with a dual-channel (Nicolet 4094C) digital oscilloscope. Gas mixtures and reactant pressures were measured with an MKS Baratron capacitance manometer.

Cl-atom Detection: The Cl-atom resonance lamp used in the experiments has been described in previous works [5–7] and is similar to that discussed by Whytock et al. [14] and Clyne and Nip. [15] The lamp was operated at 50 Watts microwave power in a mixture containing 1×10^{-3} of Cl_2 in helium. The flowing pressure in the lamp was 1.5 Torr. This configuration gives a multiplet (133.6–139.6 nm) structure that is somewhat

reversed. Resonance radiation was observed through a BaF_2 crystal window filter without wavelength resolution. A typical experimental record is shown in Fig. 1 where a decreasing ARAS signal results after the CH_2Cl_2 sample has been shock-heated. The fraction of light that is Cl-atom resonance radiation was determined earlier in CCl_4 experiments. [5,6] These indicated that 86(±2)% of the light is resonance radiation. Since this fraction is known, absorbance by Cl-atoms can be determined from the expression, $(ABS)_t \equiv -\ln \frac{I_t}{I_o}$.

In earlier work from this laboratory, the curve-of-growth for Cl-atoms has been established from the measurements of long time steady-state absorptions of Cl-atoms from the thermal decomposition of CH_3Cl. [5] The result of these experiments can be expressed in a modified form of Beer's law, $T_\infty = \frac{I_\infty}{I_o} = \exp(-K[Cl]^p)$. When [Cl] is expressed in units of atoms cm^{-3}, the values of K and p were deduced giving

$$(ABS)_\infty = 4.41 \times 10^{-9} [Cl]^{0.581}. \quad (3)$$

This result has been corroborated by subsequent experiments using CF_3Cl as the source of Cl atoms. [16] Since secondary reactions of Cl with the substrate are no longer possible, the Cl-atom absorption signal unambiguously points to the complete dissociation of the CF_3Cl molecules. These independent experiments yielded results that were in complete agreement with equation (3); thus, confirming the conclusions from the CH_3Cl study. Using the expression from Eqn. (3), the measured Cl-atom absorbance profiles, $(ABS)_t$, can be easily converted to Cl-atom concentrations, $[Cl]_t$.

Gases: The high purity He (99.995%), used as the driver gas, was obtained from Air Products and Chemicals, Inc. Scientific grade Kr (99.997%), used as the diluent gas in reactant mixtures, was obtained from MG Industries. Airco Industrial Gases supplied the ultra-high purity grade He (99.999%) used in the resonance lamp. Research grade Cl_2 (99.999%) was obtained from MG Industries and was used as received. Analytical grade

CH_2Cl_2 was obtained from Mallinckrodt Specialty Chemicals Co. and was purified by bulb-to-bulb distillation, retaining only the middle third, before use. The sample was further subjected to mass spectrometric analysis to verify its purity.

RESULTS

Fifty-two experiments were performed at three different loading pressures and at temperatures between 1400–2300 K under the conditions given in Table 1. Using Eqn. (3), the measured absorption signals were converted to $[Cl]_t$. A typical result is shown in Fig. 2. We found that [Cl] always increased rapidly to a near steady-state value; however, depending on temperature, there was a subsequent small increase in concentration that could extend over several tenths of milliseconds after the initial rapid rise. Unlike all earlier studies from this laboratory, [5-7,16] the maximum [Cl] never came close to equaling the initial reactant concentration; i. e., if the experiment shown in Fig. 2 had been carried out with the same rate of formation using CF_3Cl instead of CH_2Cl_2, then the dashed line in the figure would have been observed. This depressed yield of [Cl] immediately means that some reaction or reactions serve to perturb the reaction away from unit stoichiometry.

In order to understand the possible reaction perturbations that might explain the depressed yields, the mechanism shown in Table 2 was numerically integrated. With the small $[CH_2Cl_2]_0$ used in the experiments (Table 1), reactions (3), (4), and (7) of Table 2 contribute negligibly to the [Cl] profile under all conditions. If these reaction rate constants are set to zero, the resulting predictions of $[Cl]_t$ change at most by a few percent under all conditions. Apparently, the major process that perturbs the reaction from unit stoichiometry is reaction (1), the molecular elimination channel. The long time slow buildup of [Cl] is formally attributed to the chloromethyl-radical decompositions, reactions (5) and (6) in Table 2; however, it should be noted that if reaction (3) is negligible then reaction (6) is likewise unimportant. We also investigated the possibility that both self- and cross- recombination and disproportionation reactions of these chloromethyl-radicals

might contribute. There are a total of nine such reactions, and Bozzelli and coworkers [8] have theoretically determined rate constants for these processes. With their estimates, our conclusion is that these reactions are also negligible under the low concentration conditions of the present study. Hence, all of the present experiments can be explained by fitting the observed profiles to three rate constants, (1), (2), and (5); however, even though the contributions of reactions (3), (4), (6), and (7) are minimal, they are included in the final simulations.

In order to determine rate constants, the Table 2 mechanism was numerically integrated with various values for k_1, k_2, and k_5. The predicted Cl-atom profiles were then compared to experiment. Since the values for k_5 were generally less than $0.2(k_1 + k_2)$, the long time buildup is effectively weakly coupled to the rates for (1) and (2). Hence, the values for k_1 and k_2 could be easily determined by mutual adjustment until the short time rapid buildup matched the experiment. The solid line in Fig. 2 shows a typical fit for the first-order values given in the figure caption. Anticipating that the reactions will be nearly second-order, we have reported second-order rate constants in Table 1 for the entire range of experimental conditions. The results for k_1/[Kr] and k_2/[Kr] from Table 1 are plotted in Arrhenius form in Figs. 3 and 4, respectively. Linear-least squares analysis gives,

$$k_1/[\mathrm{Kr}] = 2.26 \times 10^{-8} \exp(-29007\ \mathrm{K/T})\ \mathrm{cm^3\ molecule^{-1}\ s^{-1}}, \quad (4)$$

and,

$$k_2/[\mathrm{Kr}] = 6.64 \times 10^{-9} \exp(-28404\ \mathrm{K/T})\ \mathrm{cm^3\ molecule^{-1}\ s^{-1}}. \quad (5)$$

The points shown in the two figures deviate by ±43% and ±40% from Eqns. (4) and (5), respectively, at the one standard deviation level. The expression for the atomic elimination reaction (5) is identical within experimental error to that for CH_3Cl decomposition, $1.09 \times 10^{-8} \exp(-29325\ \mathrm{K/T})\ \mathrm{cm^3\ molecule^{-1}\ s^{-1}}$ (1600-2100 K), over the common range of temperature overlap. [5]

DISCUSSION

In earlier studies from this laboratory on CH_3Cl [5] and CF_3Cl, [16] molecular elimination in competition with atomic elimination was not observed. In the $COCl_2$ decomposition study, [7] molecular elimination was observed; however, it amounted to only about 10% of the total decomposition. These results could be easily rationalized in terms of thermochemistry because the molecular processes were more endothermic than atomic elimination in all cases except $COCl_2$ where the threshold energy was substantially higher than the ΔH_0° making molecular elimination less likely than simple atomic dissociation. In the present case it is obvious by inspection of Eqns. (4) and (5) that molecular elimination is dominating over atomic elimination. This may mean that the two processes occur at roughly the same threshold energy indicating the need for a careful assessment of the thermochemistry for the two channels.

There are three critical evaluations of thermochemical data for the species involved in reactions (1) and (2). The Janaf tables [19] give thermodynamic functions for CH_2Cl_2, CHCl, and HCl whereas values for CHCl and CH_2Cl are listed by Manion and Rodgers [20]. Lias et al. [21] have reported $\Delta_f H_0^\circ$ values from appearance potential measurements for all species. There is a $\Delta_f H_0^\circ$ discrepancy for CHCl between Janaf (79.8 kcal $mole^{-1}$) and the other two compilations (70.9 kcal $mole^{-1}$). Hence, ΔH_{10}° ranges between 79.0 (Janaf) and 70.1 kcal $mole^{-1}$ (Manion and Rodgers, Lias et al.). For CH_2Cl, Manion and Rodgers give $\Delta_f H_0^\circ$ = 29.25 kcal $mole^{-1}$; however, this value is probably only accurate to ±1–2 kcal $mole^{-1}$. Using this value, ΔH_{20}° = 79.04 kcal $mole^{-1}$, indicating that the molecular elimination channel may be lower lying than atomic elimination depending on the barrier height for the reverse reaction (-1).

Reactions (1) and (2) have been theoretically analyzed by using the semi-empirical Troe theoretical formalism. [22–24] As in earlier studies, [7,16] we fitted the experimental data by allowing variations in both E_0° and ΔE_{down}. The latter quantity specifies the collisional deactivation efficiency factor, β_c.

To our knowledge, the barrier height for reaction (1) has never been estimated from electronic structure calculations. It has therefore been necessary to construct a fairly rigid transition state for this process by empirical methods. $k_{1\infty}$, which is dependent on E°_{10}, can then be calculated by conventional transition state methods. The calculation of k^{sc}_{10}/Z_{LJ} is unambiguous [22-24] and follows procedures described earlier. [5,7] Z_{LJ} for CH_2Cl_2 + Kr collisions is evaluated from Lennard-Jones parameters as determined from polarizabilities estimated from procedures described by Hirschfelder, Curtiss, and Bird [25] along with the method of Cambi et al. [26] for obtaining σ_{12} and ε_{12}/k. With molecular parameters for CH_2Cl_2 taken from Janaf, several theoretical calculations were performed as functions of both E°_{10} and ΔE_{1down}. The best fit was obtained with values (73.0 kcal mole^{-1}, 630 cm^{-1}); however, (75.0, 874) and (71.0, 394) also gave acceptable fits. The Troe fit parameters are shown in Table 3 for (73.0, 630), and the predicted bimolecular rate constants are plotted in Fig. 5 in comparison to the data at the three loading pressures.

If the back reaction (-1) is assumed to have a zero barrier height, then E°_{10} would be equal to ΔH°_{10}. Use of the previously mentioned Janaf value, ΔH°_{10} =79.0 kcal mole^{-1}, requires an unreasonably high value for ΔE_{1down} and gives fits that are much too steep and not a good representation of the data. Acceptance of the value implied by Manion and Rodgers, ΔH°_{10} = 70.1 kcal mole^{-1}, would be compatible with the present results but would imply a barrier height for the reverse process of 2.9 kcal mole^{-1}. Also, with E°_{10} = 73.0 kcal mole^{-1}, the values for K_{1eq} and the high pressure rate constant for reaction (1) are, respectively,

$$K_{1eq} = 1.135 \times 10^{26} \exp(-33694\ K/T) \text{ molecules cm}^{-3}\ (\pm 3\% \text{ at } 1\sigma), \qquad (6)$$

and,

$$k_{1\infty} = 3.10 \times 10^{14} \exp(-38053\ K/T)\ s^{-1}\ (\pm 1\% \text{ at } 1\sigma) \qquad (7)$$

for the temperature range, 1400-2300 K. Equation (7) divided by (6) gives an apparent high pressure activation energy for the back reaction of about 8.7 kcal mole^{-1}, but Eqn. (6) can also be divided into the calculated values for k_1/[Kr] to predict values for k_{-1}/[Kr]. For 11 Torr loading pressure, between 1400-2300 K,

$$k_{-1}/[Kr] = 9.12 \times 10^{-25} T^{-2.62} \text{ cm}^6 \text{ molecule}^{-2} \text{ s}^{-1}. \quad (8)$$

Since theory fits experiment (Fig. 5), similar values can be obtained by dividing Eqn. (6) into the experimental result, (4).

$$k_{-1}/[Kr] = 1.99 \times 10^{-34} \exp(4687 \text{ K/T}) \text{ cm}^6 \text{ molecule}^{-2} \text{ s}^{-1}. \quad (9)$$

At this pressure, either expression, (8) or (9), shows a negative T-dependence indicating that the reaction is nearer to the third- than the second-order limit and also that much of the T-dependence is carried in the β_c factor. This point is corroborated by comparing theoretical k_1/[Kr] to $\beta_c \frac{k_{10}^{\infty}}{[Kr]}$. The former varies from 21 to 48 % of the latter over the temperature range showing that reaction (1) is nearer to the second- than the first-order limit.

Troe calculations have also been performed to understand reaction (2). Though earlier values of molecular parameters for CH_2Cl have been reported and have been used for thermodynamic function evaluation, [20] here we have elected to use recent electronic structure results from Harding [27] with the vibrations slightly scaled to reflect certain observed frequencies. These calculations show that the structure is slightly bent from a planar configuration. We have calculated the absolute entropy for CH_2Cl and find that the new calculation is only ~1.2% higher at all temperatures than that of Manion and Rodgers. Harding's estimation for $\Delta_f H_0^\circ$ is only approximate, and therefore, we have again performed calculations with both E_{20}° and ΔE_{2down} as parameters. As before, [5,7] k_{-2LJ}

was calculated with a Lennard-Jones collision model from estimated CH_2Cl polarizabilities [25] using the method of Cambi et al. [26] The result between 1400 and 2300 K is $k_{-2LJ} = (5.44 \pm 0.15) \times 10^{-11}$ cm^{-3} molecule^{-1} s^{-1}. The experimental rate constants were then compared to Troe calculations at mutual values of E°_{20} and ΔE_{2down} ranging from 81.25 kcal mole^{-1} and 560 cm^{-1}, respectively, to 75.25 and 268. All fits were acceptable with the one at 78.25 and 394 being only slightly superior at all pressures. This latter calculation is shown in Table 4 and is plotted with the data in Fig. 6. Between 1400 and 2300 K, the calculated equilibrium constant can be expressed to within ±2% by,

$$K_{2eq} = 2.203 \times 10^{26} \exp(-38822\ K/T) \text{ molecules cm}^{-3}. \quad (10)$$

The value for high pressure limiting rate constant is,

$$k_{2\infty} = 1.33 \times 10^{16} \exp(-39017\ K/T)\ s^{-1}\ (\pm 2\% \text{ at } 1\sigma). \quad (11)$$

Reaction (2) is also predicted to be near the low pressure limit as shown by comparing theoretical $k_2/[Kr]$ to $\beta_c \frac{k^{sc}_{20}}{[Kr]}$. In this case, the former ranges from 65 to 74% of the latter over the temperature range.

Lastly, theoretical calculations have been carried out to see whether the values for k_5 that are specified from the experimental fits, are reasonable. This reaction will undoubtedly be in the low pressure limit, and therefore, we have estimated $\beta_c \frac{k^{sc}_{50}}{[Kr]}$ using $E^{\circ}_{50} = \Delta H^{\circ}_{50} =$ 92.6 kcal mole^{-1}. The predicted T-dependence is generally too steep; however, the magnitudes for k_5 in the middle range of temperature can be justified with values of β_c between 0.55 and 0.72 .

In conclusion, the main finding from this study is that the molecular elimination process in the thermal decomposition of CH_2Cl_2 predominates over the atomic process.

This conclusion suggests that the Janaf value for the heat of formation for CHCl is overestimated, but the value given by Manion and Rodgers is compatible with the present result. The heat of formation for CH_2Cl from Manion and Rodgers might be high by ~0.8 kcal $mole^{-1}$; however, the present conclusion is clearly only accurate to ~±3 kcal $mole^{-1}$, and this is higher than the uncertainty in their estimate. Second, we find relatively large values for ΔE_{down} in both (1) and (2). For best fits it has been necessary to use different values for the two reactions, and this may suggest that energy transfer from the activated molecule may be dependent on total energy.

Acknowledgment: The authors wish to thank Drs. A. F. Wagner, L. B. Harding, and J. P. Hessler for a thorough reading of the manuscript and helpful suggestions. This work was supported by the U. S. Department of Energy, Office of Basic Energy Sciences, Division of Chemical Sciences, under Contract No. W-31-109-Eng-38.

References

1 Graham, J. L., Hall, D. L., and Dellinger, B., *Environ. Sci. Tech.* 20:703–710 (1986).

2 Oppelt, E. T., *J. Air Poll. Contr. Assoc.* 37:558–586 (1987).

3 Senkan, S. M., *Environ. Sci. Tech.* 22:368–370 (1988).

4 Hart, J. R., and Franco, G., *Proceedings of the Third Symposium on the Incineration of Hazardous Wastes*, San Diego, CA, 1989, Paper 15.

5 Lim, K. P., and Michael, J. V., *J. Chem. Phys.* 98:3919–3928 (1993).

6 Michael, J. V., Lim, K. P., Kumaran, S. S., and Kiefer, J. H., *J. Phys. Chem.* 97:1914–1919 (1993).

7 Lim, K. P., and Michael, J. V., *J. Phys. Chem.*, submitted.

8 Ho, W., Barat, R. B., and Bozzelli, J. W., *Combust. Flame* 88:265–295 (1992).

9 Ho. W., and Bozzelli, J. W., *Twenty-Fourth Symposium (International) on Combustion*, The Combustion Institute, Pittsburgh, 1992, pp. 743–748.

10 Dean, A. M., *J. Phys. Chem.* 89:4600–4608 (1985).

11 Westmoreland, P. R., and Dean, A. M., *AIChE J.* 32:1971–1979 (1986).

12 Michael, J. V., *Prog. Energy Combust. Sci.* 18:327–347 (1992), and references cited therein.

13 Michael, J. V., and Sutherland, J. W., *Int. J. Chem. Kinet.* 18:409–436 (1986).

14 Whytock, D. A., Lee, J. H., Michael, J. V., Payne, W. A., and Stief, L. J., *J. Chem. Phys.* 66:2690–2695 (1977).

15 Clyne, M. A. A., and Nip, W. S., *J. Chem. Soc. Faraday II*, 72:838-847 (1976).

16 Kiefer, J. H., Sathyanarayana, R., Lim, K. P., and Michael, J. V., *J. Phys. Chem.*, submitted.

17 Based on, DeMore, W. B., Sander, S. P., Golden, D. M., Hampson, R. F., Kurylo, M. J., Howard, C. J., Ravishankara, A. R., Kolb, C. E., and Molina, M. J., *Chemical Kinetic and Photochemical Data for use in Stratospheric Modeling*, Evaluation No. 10, JPL Publication 92-20, August 15, 1992.

18 Seery, D. J. and Bowman, C. T., *J. Chem. Phys.* 48:4314-4317 (1968).

19 Chase, M. W. Jr., Davies, C. A., Downey, J. R. Jr., Frurip, D. J.,McDonald, R. A., and Syverud, A. N., *J. Phys. Chem. Ref. Data* 14:Supplement No. 1 (1985).

20 Manion, J. A. and Rodgers, A. S., *Thermodynamic Tables, Non-Hydrocarbons*, Thermodymaics Research Center, Texas A & M University Press, College Station, TX, June 30, 1993, p. r-7250 – r-ref-7251.

21 Lias, S. G., Bartmess, J. E., Liebman, J. F., Holmes, J. L., Levin, R. D., and Mallard, W. G., *J. Phys. Chem. Ref. Data* 17:Supplement No. 1 (1988).

22 Troe, J., *J. Chem. Phys.* 65:4745–4757 (1977); *ibid.* 4758–4775 (1977).

23 Troe, J., *J. Phys. Chem.* 83:114–126 (1979).

24 Troe, J., *Ber. Bunsenges. Phys. Chem.* 87:161–169 (1983); Gilbert, R. G., Luther, K. and Troe, J., *ibid.* 169-177 (1983)

25 Hirschfelder, J. O., Curtiss, C. F., and Bird, R. B., *Molecular Theory of Gases and Liquids*, Wiley: New York, 1966, p 951.

26 Cambi, R., Cappelletti, D., Liuti, G., and Pirani, F., *J. Chem. Phys.* 95: 1852-1861 (1991).

27 Harding, L. B., private communication, September, 1993.

Table 1. Rate Data for the CH_2Cl_2 Decomposition Reactions.

P Torr	Mach #	ρ 10^{18} cm^{-3}	Temp K	k_1/[Kr] cm^{3}molecule^{-1}s^{-1}	k_2/[Kr] cm^{3}molecule^{-1}s^{-1}
		$X_{CH_2Cl_2} = 7.642 \times 10^{-6}$			
15.94	2.868	3.423	1994	1.120×10^{-14}	4.141×10^{-15}
16.00	2.825	3.402	1933	9.919×10^{-15}	3.306×10^{-15}
15.87	2.912	3.451	2042	1.375×10^{-14}	5.086×10^{-15}
15.93	2.722	3.291	1807	4.579×10^{-15}	1.650×10^{-15}
15.99	2.627	3.209	1695	1.449×10^{-15}	4.830×10^{-16}
15.87	2.398	2.930	1440	2.990×10^{-17}	1.106×10^{-17}
15.95	2.444	2.999	1489	5.598×10^{-17}	2.070×10^{-17}
15.99	2.514	3.088	1567	1.891×10^{-16}	6.996×10^{-17}
15.97	2.616	3.193	1682	1.086×10^{-15}	4.017×10^{-16}
15.99	2.767	3.347	1861	5.881×10^{-15}	2.066×10^{-15}
10.94	2.837	2.362	1964	1.185×10^{-14}	5.080×10^{-15}
10.94	2.622	2.208	1697	9.105×10^{-16}	4.485×10^{-16}
10.93	2.711	2.264	1881	3.710×10^{-15}	1.590×10^{-15}
10.93	2.526	2.122	1590	2.910×10^{-16}	1.567×10^{-16}
10.97	2.471	2.085	1528	1.247×10^{-16}	6.715×10^{-17}
		$X_{CH_2Cl_2} = 1.552 \times 10^{-5}$			
10.94	2.742	2.297	1843	5.245×10^{-15}	1.940×10^{-15}
10.98	2.873	2.395	2010	1.136×10^{-14}	5.344×10^{-15}
10.92	2.881	2.379	2029	1.115×10^{-14}	5.245×10^{-15}
10.95	2.715	2.271	1916	3.258×10^{-15}	1.145×10^{-15}
10.93	2.630	2.204	1713	1.565×10^{-15}	5.217×10^{-16}
10.98	2.556	2.157	1625	4.521×10^{-16}	1.507×10^{-16}
10.92	2.385	2.001	1432	5.247×10^{-17}	1.749×10^{-17}
10.88	2.471	2.067	1527	1.229×10^{-16}	6.047×10^{-17}
10.94	2.598	2.181	1674	6.464×10^{-16}	2.155×10^{-16}
10.99	2.698	2.267	1795	2.322×10^{-15}	8.159×10^{-16}
10.95	2.716	2.272	1818	4.929×10^{-15}	2.112×10^{-15}

Table 1. (Continued)

P Torr	Mach #	ρ 10^{18} cm^{-3}	Temp K	k_1/[Kr] cm^{3}molecule^{-1}s^{-1}	k_2/[Kr] cm^{3}molecule^{-1}s^{-1}
15.91	2.950	3.479	2099	9.598×10^{-15}	4.312×10^{-15}
15.89	2.825	3.357	1946	6.763×10^{-15}	3.039×10^{-15}
15.90	2.644	3.198	1721	9.179×10^{-16}	4.941×10^{-16}
15.94	2.496	3.047	1552	1.313×10^{-16}	7.055×10^{-17}
15.96	2.443	2.980	1498	3.255×10^{-17}	1.745×10^{-17}
15.93	2.591	3.138	1665	4.971×10^{-16}	2.677×10^{-16}
15.88	2.717	3.255	1814	4.486×10^{-15}	1.659×10^{-15}
15.87	2.784	3.327	1889	7.689×10^{-15}	3.264×10^{-15}
15.88	2.713	3.262	1803	2.504×10^{-15}	8.936×10^{-16}
15.96	2.493	3.052	1553	1.392×10^{-16}	5.734×10^{-17}
		$X_{CH_2Cl_2} = 1.571 \times 10^{-5}$			
5.96	3.064	1.355	2283	3.099×10^{-14}	1.033×10^{-14}
5.92	2.824	1.269	1954	9.099×10^{-15}	3.545×10^{-15}
5.96	2.684	1.224	1778	2.451×10^{-15}	8.170×10^{-16}
5.92	2.474	1.126	1531	8.879×10^{-17}	3.107×10^{-17}
5.92	2.573	1.170	1644	4.274×10^{-16}	1.881×10^{-16}
5.93	2.679	1.212	1778	2.352×10^{-15}	7.840×10^{-16}
5.95	2.887	1.294	2043	1.758×10^{-14}	5.408×10^{-15}
5.95	2.921	1.306	2088	1.421×10^{-14}	5.168×10^{-15}
5.97	2.988	1.338	2171	2.809×10^{-14}	9.717×10^{-15}
5.96	2.619	1.193	1705	5.028×10^{-16}	3.771×10^{-16}
5.94	2.826	1.270	1963	1.010×10^{-14}	5.314×10^{-15}
5.90	2.701	1.214	1804	2.450×10^{-15}	1.400×10^{-15}
5.95	2.615	1.190	1700	2.101×10^{-15}	8.826×10^{-16}
5.94	2.359	1.072	1408	2.798×10^{-17}	1.119×10^{-17}
5.97	2.455	1.123	1514	9.792×10^{-17}	5.786×10^{-17}
5.97	2.695	1.227	1798	1.329×10^{-15}	1.019×10^{-15}

Table 2. The Mechanism for the Decomposition of CH_2Cl_2.

(1)	$CH_2Cl_2 \rightarrow CHCl + HCl$	k_1 = to be fitted
(2)	$CH_2Cl_2 \rightarrow CH_2Cl + Cl$	k_2 = to be fitted
(3)	$Cl + CH_2Cl_2 \rightarrow CHCl_2 + HCl$	$k_3 = 6 \times 10^{-11} \exp(-1615\ K/T)$[a]
(4)	$CHCl + CH_2Cl_2 \rightarrow C_2H_3Cl_3$	$k_4 = 2.5 \times 10^{-11}$ [b]
(5)	$CH_2Cl \rightarrow CH_2 + Cl$	k_5 = to be fitted[c]
(6)	$CHCl_2 \rightarrow CHCl + Cl$	k_6 = to be fitted[c]
(7)	$HCl + Kr \rightarrow H + Cl + Kr$	$k_7 = 6.97 \times 10^{-11} \exp(-40765\ K/T)$[d]

[a]Value based on reference 17. Units are cm^3 $molecule^{-1}$ s^{-1}. [b]Estimated. Units are cm^3 $molecule^{-1}$ s^{-1}. [c]k_5 and k_6 are taken to be equal. [d]Reference 18

TABLE 3. Parameters for the theoretical evaluation of $CH_2Cl_2 \rightarrow CHCl + HCl$[a]

T /K	F_{anh}	F_{rot}	F_E	$\frac{k_{10}^{sc}}{[Kr]}$/cm^3 molecule^{-1} s^{-1}	S_K	B_K	β_c	$F(k_0/k_\infty)$[b]
1400	1.47	1.811	1.312	8.42(-16)[c]	5.40	12.4	0.109	0.283
1500	1.47	1.783	1.340	3.83(-15)	5.56	12.3	0.096	0.296
1600	1.47	1.754	1.370	1.40(-14)	5.70	12.1	0.086	0.314
1700	1.47	1.726	1.400	4.31(-14)	5.84	11.9	0.076	0.336
1800	1.47	1.698	1.432	1.15(-13)	5.97	11.7	0.068	0.360
1900	1.47	1.669	1.464	2.70(-13)	6.08	11.6	0.060	0.385
2000	1.47	1.642	1.498	5.76(-13)	6.19	11.4	0.054	0.411
2100	1.47	1.614	1.533	1.12(-12)	6.29	11.1	0.048	0.436
2200	1.47	1.586	1.570	2.03(-12)	6.39	10.9	0.043	0.461
2300	1.47	1.559	1.607	3.45(-12)	6.48	10.7	0.039	0.484

[a] E_1° = 73.0 kcal mole^{-1} and ΔE_{1down} = 630 cm^{-1}. The Janaf molecular parameter values for CH_2Cl_2 give $\rho(E_0)$ = 3143 states/cal mole^{-1} at the threshold energy. [b]Evaluated at 11 Torr loading pressure. [c]Denotes the power of ten.

TABLE 4. Parameters for the theoretical evaluation of $CH_2Cl_2 \rightarrow CH_2Cl + Cl$[a]

T /K	F_{anh}	F_{rot}	F_E	$\frac{k_{20}^{sc}}{[Kr]}$/cm^3 molecule^{-1} s^{-1}	S_K	B_K	β_c	$F(k_0/k_\infty)$[b]
1400	1.47	1.832	1.291	2.02(-16)[c]	5.32	12.8	0.057	0.652
1500	1.47	1.806	1.317	1.04(-15)	5.45	12.5	0.050	0.662
1600	1.47	1.779	1.344	4.24(-15)	5.56	12.2	0.043	0.671
1700	1.47	1.752	1.371	1.44(-14)	5.67	11.9	0.038	0.681
1800	1.47	1.726	1.400	4.17(-14)	5.77	11.7	0.033	0.691
1900	1.47	1.699	1.430	1.06(-13)	5.87	11.4	0.030	0.700
2000	1.47	1.672	1.461	2.42(-13)	5.96	11.2	0.026	0.710
2100	1.47	1.646	1.493	5.02(-13)	6.04	10.9	0.023	0.719
2200	1.47	1.620	1.525	9.60(-13)	6.12	10.7	0.021	0.728
2300	1.47	1.594	1.559	1.72(-12)	6.19	10.5	0.019	0.737

[a] $E_2^\circ = \Delta H_{20}^\circ$ =78.25 kcal mole^{-1} and ΔE_{2down} = 394 cm^{-1}. The Janaf molecular parameter values for CH_2Cl_2 give $\rho(E_0)$ = 4958 states/cal mole^{-1} at the threshold energy. [b]Evaluated at 11 Torr loading pressure. [c]Denotes the power of ten.

Figures

Fig. 1. A typical experimental record showing decreasing ARAS signal as Cl-atoms are produced from the thermal decomposition of CH_2Cl_2. [Cl] rapidly attains a nearly steady-state value. The experimental conditions are: T = 1804 K, P = 227 Torr, $\rho = 1.214 \times 10^{18}$ cm^{-3}, and $X_{CH_2Cl_2} = 2.885 \times 10^{-5}$.

Fig. 2. The experimental profile of $[Cl]_t$ derived from Fig.1. The solid line is a simulated fit that is based on the mechanism in Table 2. The dashed line shows the [Cl] that would have been observed if molecular elimination, reaction (1), did not occur; i. e., if an equivalent experiment with CF_3Cl were performed. The solid line fit required, $k_1 = 2975$ s^{-1}, $k_2 = 1700$ s^{-1}, and $k_5 = 300$ s^{-1}

Fig. 3. The Arrhenius plot of the second-order rate constants for reaction (1) at three loading pressures (Table 1): (O) 16 Torr, (Δ) 11 Torr, and (□) 6 Torr. The solid line, Eqn. (4), is the linear least-squares fit to the data.

Fig. 4. The Arrhenius plot of the second-order rate constants for reaction (2) at three loading pressures (Table 1): (O) 16 Torr, (Δ) 11 Torr, and (□) 6 Torr. The solid line, Eqn. (5), is the linear least-squares fit to the data.

Fig. 5. A comparison of the experimental data for k_1/[Kr] to the theoretical calculations. The solid lines are calculated from the Troe's semi-empirical theory using $E^{\circ}_{10} = 73.0$ kcal mole^{-1} and $\Delta E_{1down} = 630$ cm^{-1}.

Fig. 6. A comparison of the experimental data for k_2/[Kr] to the theoretical calculations. The solid lines are calculated from the Troe's semi-empirical theory using $E^{\circ}_{20} = \Delta H^{\circ}_{20} = 78.25$ kcal mole^{-1} and $\Delta E_{2down} = 394$ cm^{-1}.

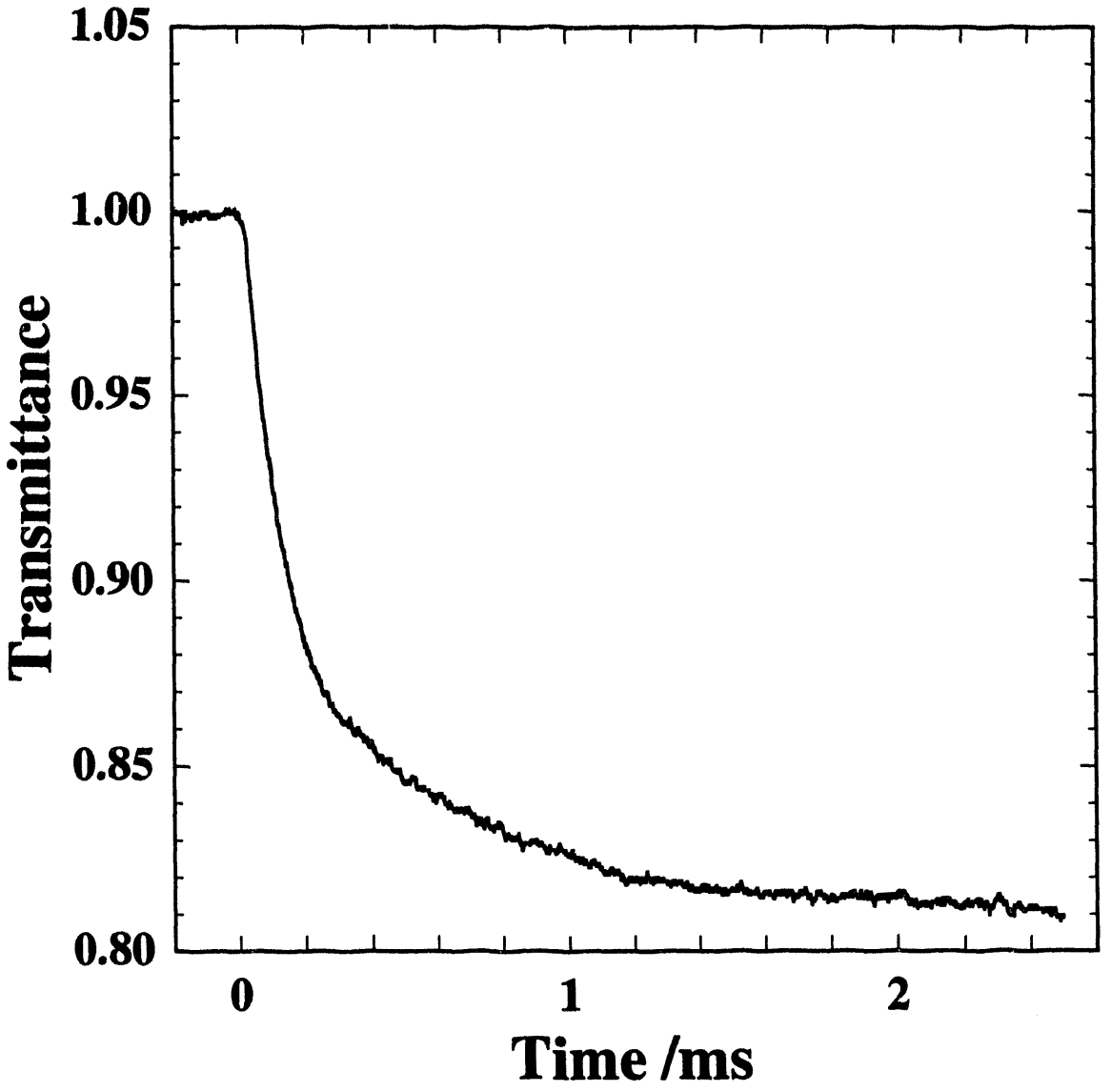

Fig. 1

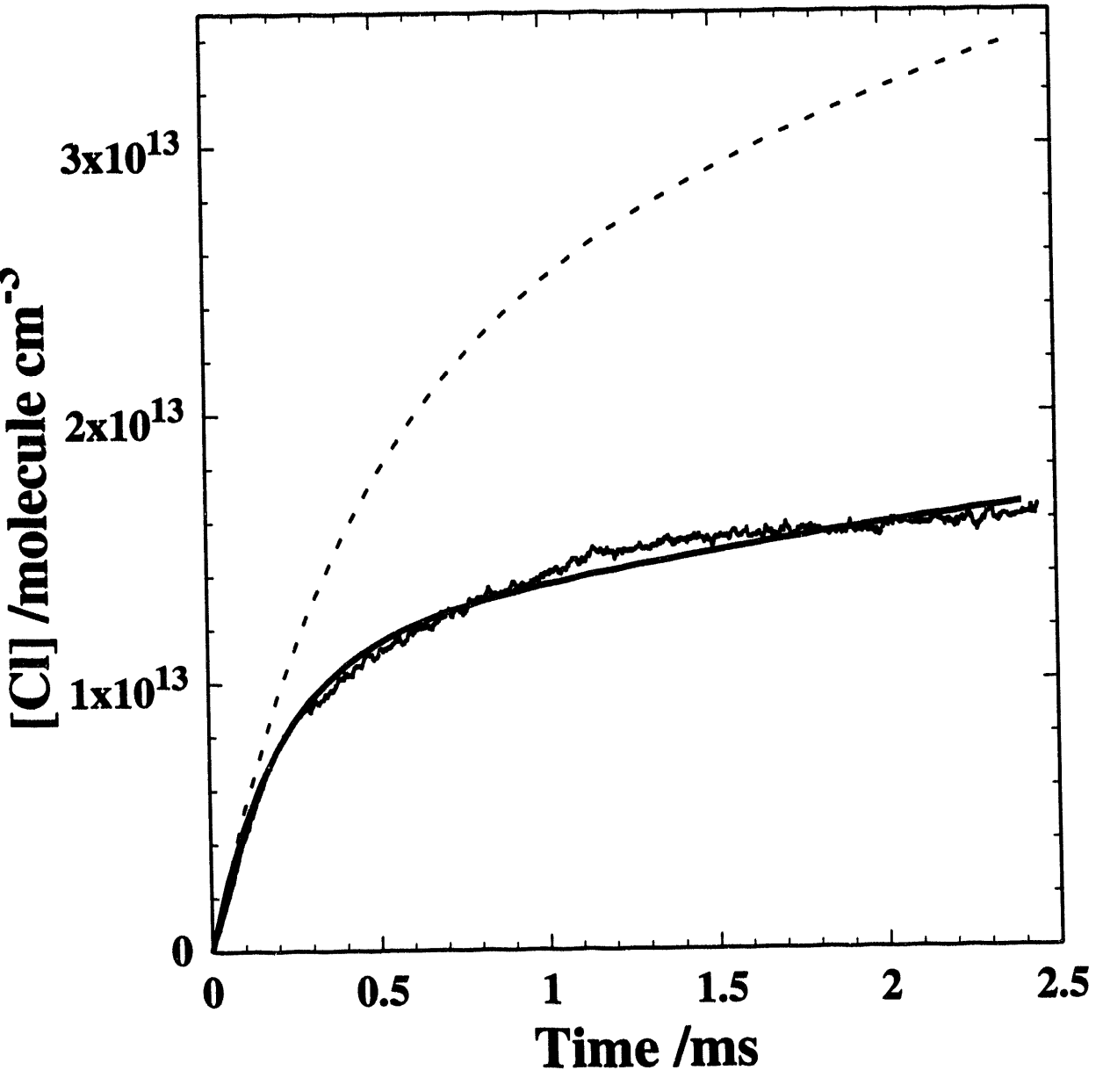

Fig. 2

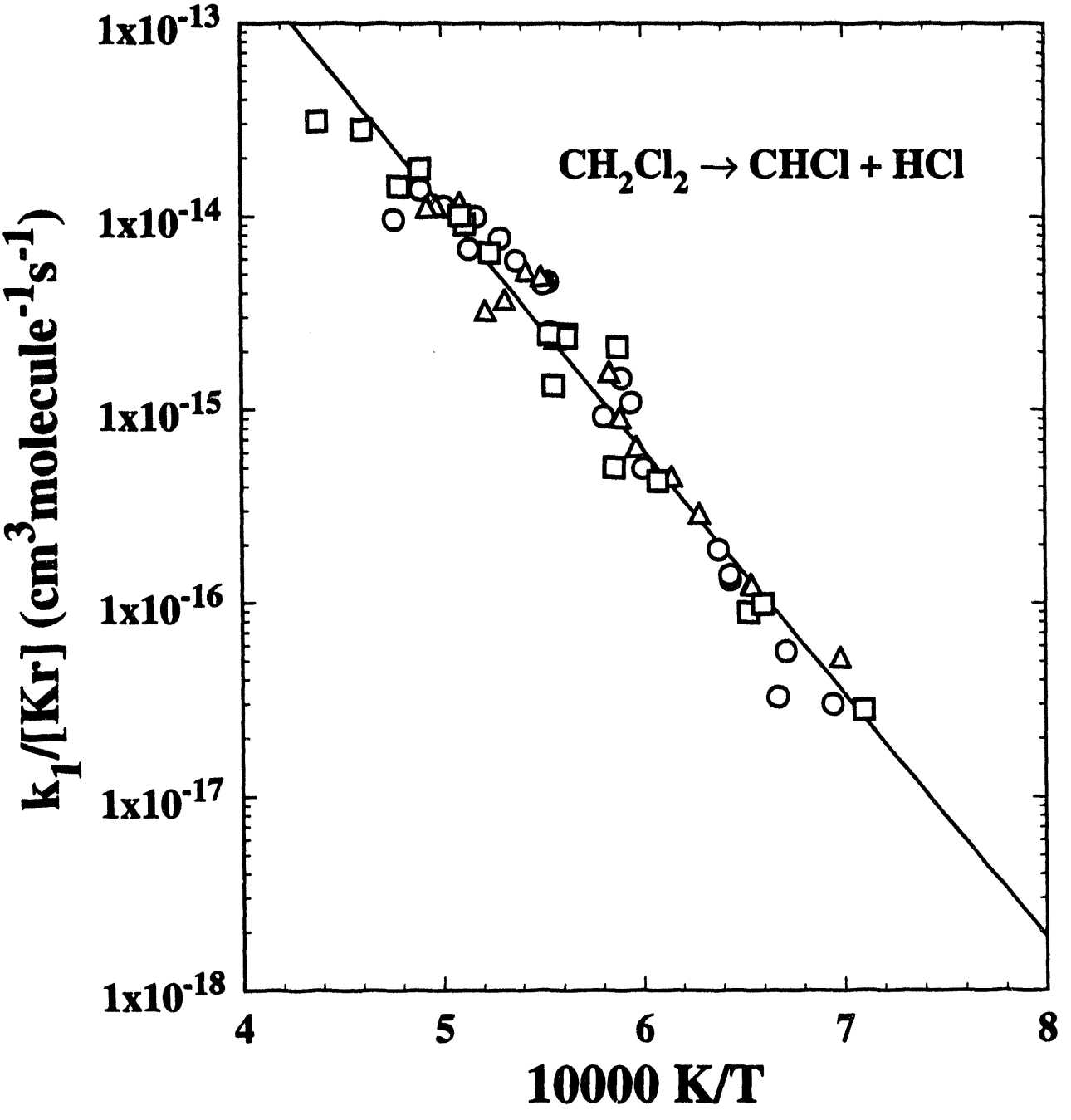
1x10-13
1x10-14
1x10-15
1x10-16
1x10-17
1x10-18
k1/[Kr] (cm3molecule-1s-1)
CH2Cl2 → CHCl + HCl
4
5
6
7
8
10000 K/T

Fig. 3

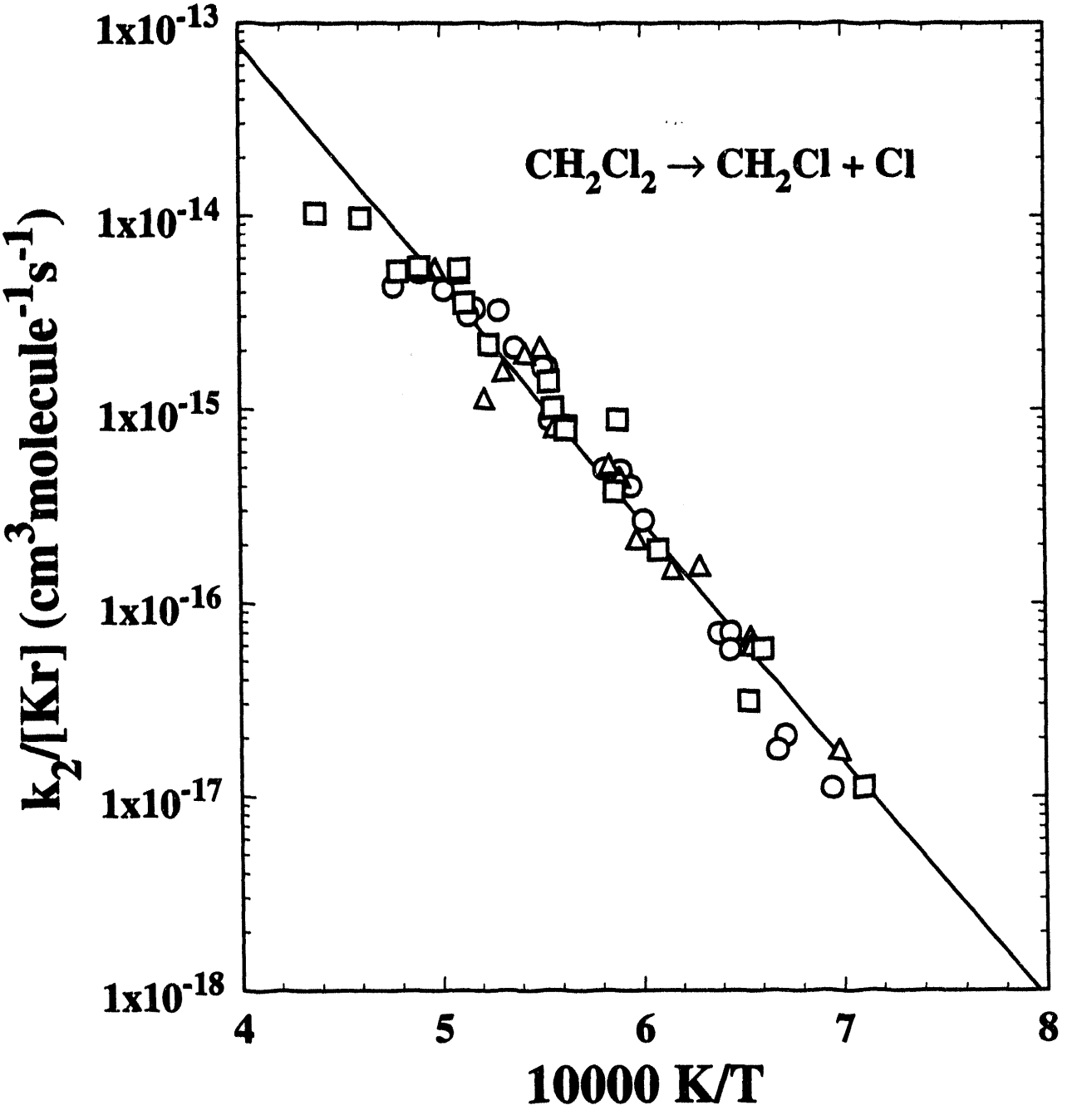
1x10-13
1x10-14
1x10-15
1x10-16
1x10-17
1x10-18
k2/[Kr] (cm3molecule-1s-1)
CH2Cl2 → CH2Cl + Cl
4
5
6
7
8
10000 K/T

Fig. 4

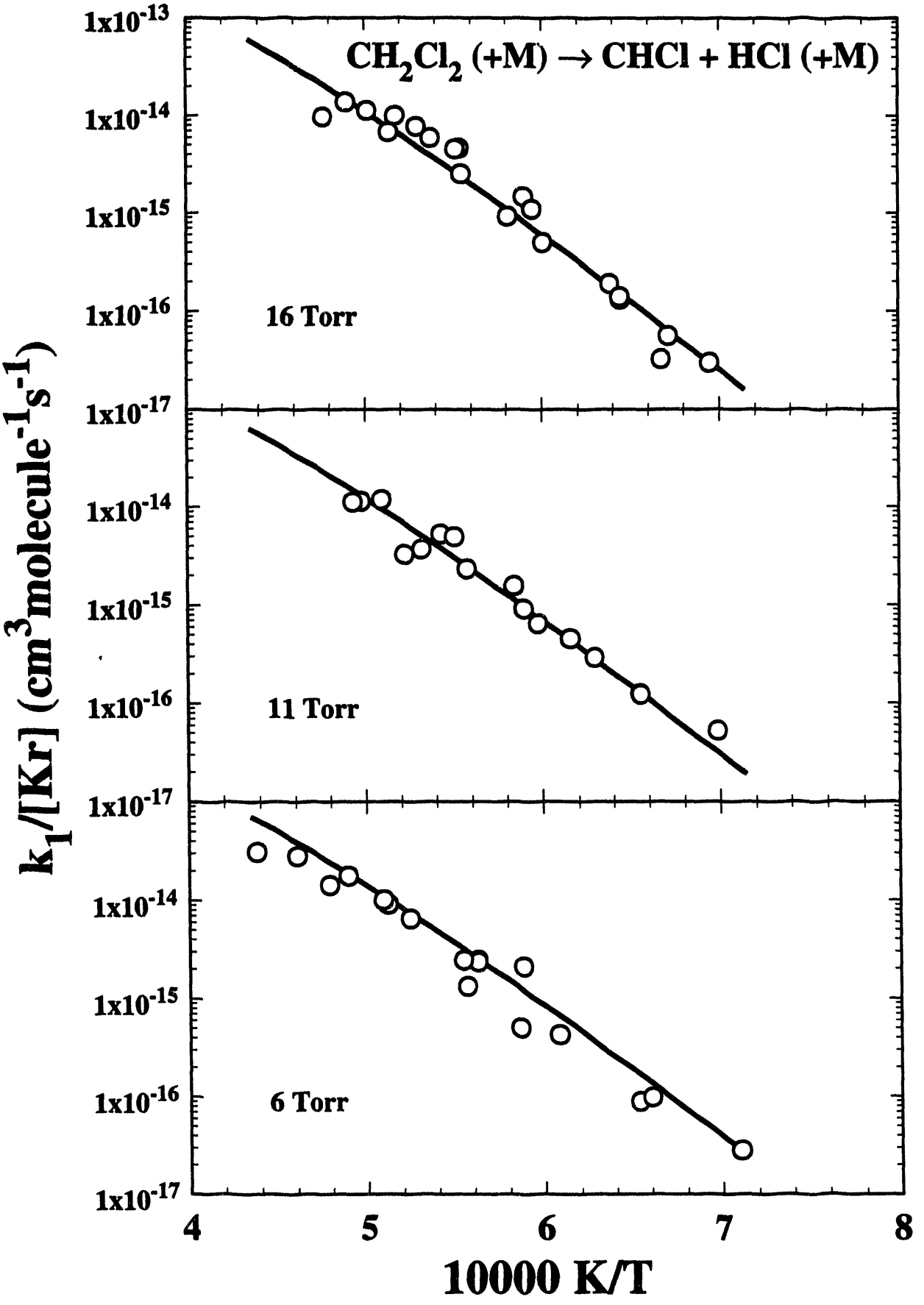
CH_2Cl_2 (+M) → CHCl + HCl (+M)
16 Torr
11 Torr
6 Torr
$k_1/[Kr]$ ($cm^3 molecule^{-1} s^{-1}$)
1x10-13
1x10-14
1x10-15
1x10-16
1x10-17
4
5
6
7
8
10000 K/T

Fig. 5

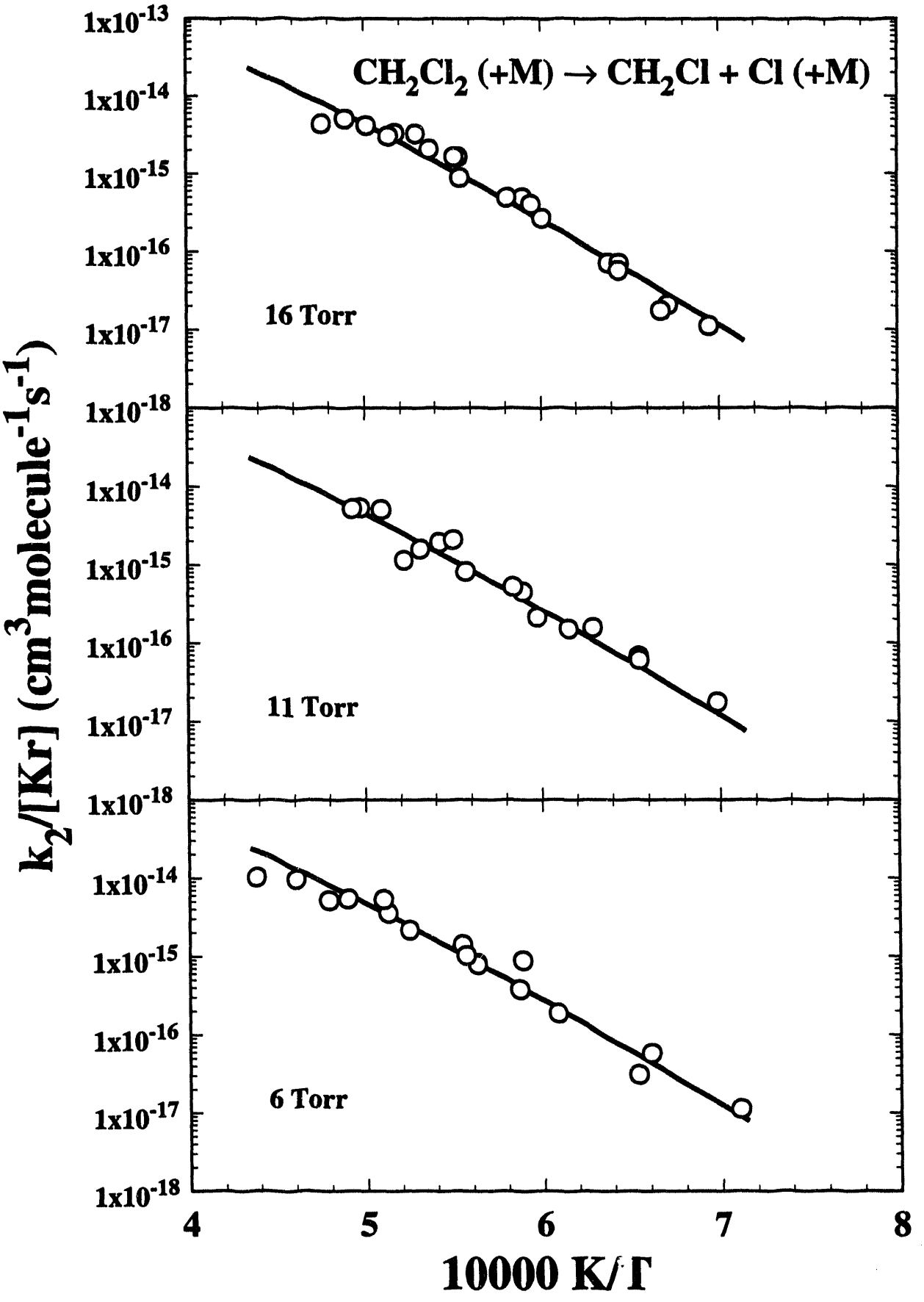
CH_2Cl_2 (+M) → CH_2Cl + Cl (+M)
16 Torr
11 Torr
6 Torr
$k_2/[Kr]$ ($cm^3 molecule^{-1} s^{-1}$)
1x10-13
1x10-14
1x10-15
1x10-16
1x10-17
1x10-18
4
5
6
7
8
10000 K/T

Fig. 6

DATE
FILMED
7/7/94

END